DOI: 10.1002/cssc.200800084

Recent Developments in Solid-State Dye-Sensitized Solar Cells

Jun-Ho Yum, Peter Chen, Michael Grätzel, and Mohammad K. Nazeeruddin*[a]

The dye-sensitized solar cell, developed in the 1990s, is a non-conventional solar technology that has attracted much attention owing to its stability, low cost, and device efficiency. Power-conversion efficiencies of over 11% have been achieved for devices that contain liquid electrolytes, whereas solid-state devices that do not require a liquid electrolyte display an overall efficiency of 5%. Improvement of the efficiency of solid-state dye-sensitized solar cells requires optimization of their various components, such as the hole-transport material, sensitizer, mesoporous TiO_2 film, and the blocking layer. This Minireview highlights the current state of the art and future directions of solid-state dye-sensitized solar cell technology.

1. Introduction

Global environmental concerns and the finite nature of fossil fuels have led to increased interest in the development of renewable energy, and solar energy has emerged as one of the best candidates in this respect. Though conventional photovoltaic devices (silicon-based solar cells) are promising for the direct conversion of photons into electrons, the prohibitive cost of these cells is uncompetitive with conventional power-generating methods. On the contrary, dye-sensitized solar cells (DSSCs) are a non-conventional photovoltaic technology that have attracted significant attention because of their high conversion efficiencies and low cost.[1–23] A typical DSSC contains five components: 1) a conductive mechanical support, 2) a semiconductor film, 3) a sensitizer, 4) an electrolyte, and 5) a counter electrode. The total efficiency of the dye-sensitized solar cell depends on the optimization and compatibility of each of these constituents.

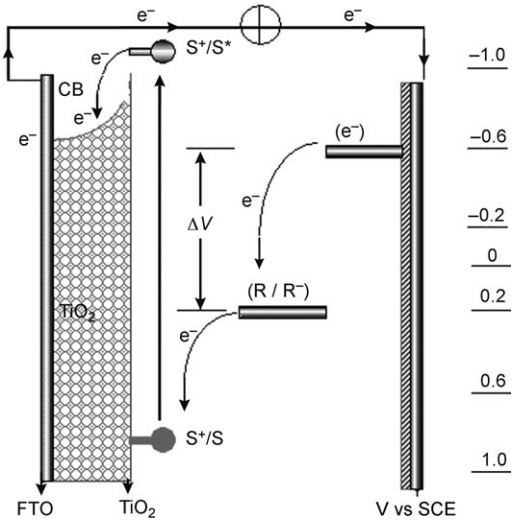

Figure 1. Operating principles and energy-level diagram of a dye-sensitized solar cell. S, S^+, and S* represent the sensitizer in the ground, oxidized, and excited state, respectively; R/R^- represents a redox mediator; CB denotes the conduction band.

The operating principle of DSSCs is shown in Figure 1. Photoexcitation of the sensitizer adsorbed on the semiconductor (S_{ads}) [Eq. (1)] leads to the injection of electrons into the conduction band of the oxide [Eq. (2)]. The oxidized dye is subsequently reduced by electron donation from the electrolyte that contains the redox system (R/R^-) [Eq. (3)]. The injected electron flows through the semiconductor network to the back contact and then through the external load to the counter electrode. At the counter electrode, the redox species are regenerated [Eq. (4)], thereby completing the circuit. With a closed external circuit and under illumination, the device then constitutes a photovoltaic energy-conversion system that is regenerative and stable. However, there are undesirable reactions that lower the device efficiency, such as the injected electrons recombining with the oxidized sensitizer [Eq. (5)] or with the oxidized redox couple at the TiO_2 surface [Eq. (6)].

$$S_{ads} + h\nu \rightarrow S^*_{ads} \quad (1)$$

$$S^*_{ads} \rightarrow S^+_{ads} + e^-_{inj} \quad (2)$$

$$S^+_{ads} + R^- \rightarrow S_{ads} + R \quad (3)$$

$$R + e^-_{cathode} \rightarrow R^-_{cathode} \quad (4)$$

$$e^-_{inj} + S^+_{ads} \rightarrow S_{ads} \quad (5)$$

$$e^-_{inj} + R \rightarrow R^-_{anode} \quad (6)$$

Photovoltaic performance data obtained with a sandwich cell under illumination by simulated AM 1.5 solar light using

[a] *Dr. J.-H. Yum, P. Chen, Prof. Dr. M. Grätzel, Dr. M. K. Nazeeruddin*
Laboratory of Photonics and Interfaces
EPFL SB ISIC LPI
CH-1015 Lausanne (Switzerland)
Fax: (+41) 21-693-4311
E-mail: mdkhaja.nazeeruddin@epfl.ch

the N719 complex are shown in Figure 2. At 1 sun, the liquid electrolyte based DSSC containing N719 as sensitizer exhibits a current density of 17.73 mA cm^{-2}, a voltage of 846 mV, and a fill factor (FF) of 0.75, yielding an overall conversion efficiency of 11.18%.[24–28] This efficiency on an active cell area of 0.158 cm^2 was validated by an accredited photovoltaic calibration laboratory, rendering the device a credible alternative to conventional p–n junction photovoltaic devices.

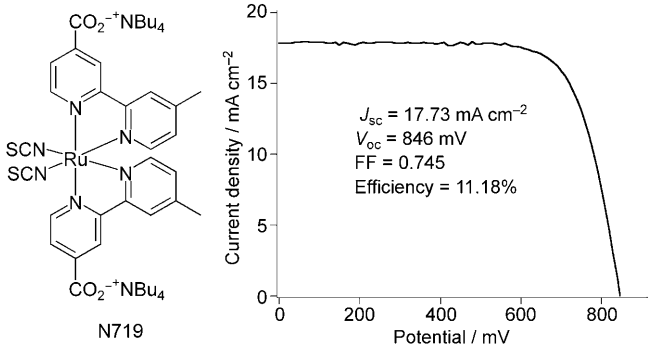

Figure 2. Current–voltage curve for a solar cell based on N719 (J_{sc} = short-circuit current density, V_{oc} = open-circuit voltage, and FF = fill factor). The conversion efficiency under AM 1.5 simulated sunlight (100 mW cm^{-2}) is 11.18%. The cell was equipped with an antireflective coating. The cell was masked with black plastic to avoid the diffusive light leaving an active cell area of 0.158 cm^2.

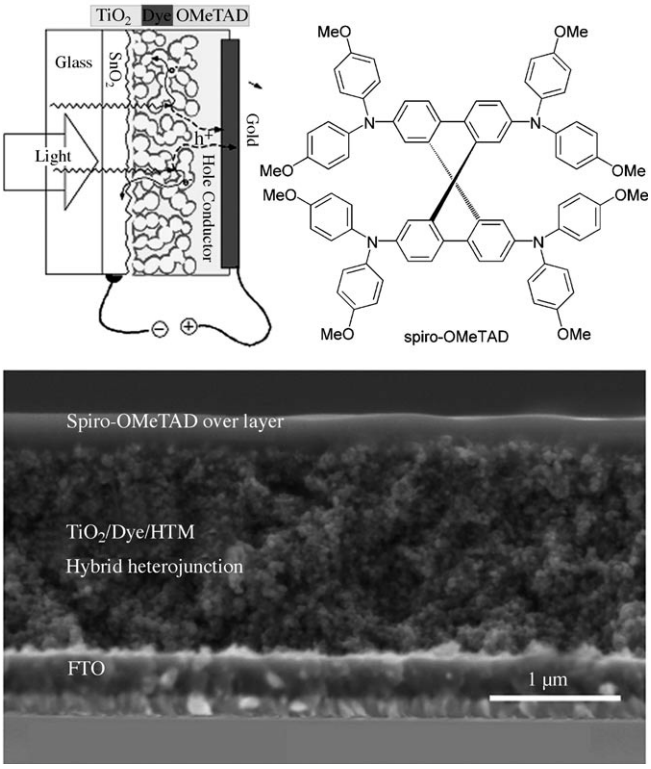

Figure 3. Cross-sectional image (top left) of a solid-state DSSC using spiro-OMeTAD as hole-transport material (HTM). The scanning electron microscopy image (bottom) shows the spiro-OMeTAD over-layer and the TiO_2/dye/HTM heterojunction on the FTO substrate.

To avoid the disadvantages of liquid electrolyte based DSSCs such as solvent evaporation and leakage, solid-state organic and inorganic hole-transport materials (HTMs) have been investigated.[29–39] Research in the area of solid-state DSSCs has gained considerable momentum during the past 10 years as they are attractive devices for manufacturing flexible photovoltaic cells by a roll-to-roll production process. Herein, we present the recent developments in solid-state DSSCs and the optical, electronic, and interfacial properties of their individual components.

2. Architecture and Fabrication Process of the Device

The basic structure of a solid-state DSSC is illustrated in Figure 3, where a hole-transport material is incorporated instead of the iodine–iodide redox couple. The use of a hole-transport material is based on the generated holes hopping towards the counter electrode. The device consists of a conducting glass substrate (fluorine-doped tin oxide, FTO), where part of the conducting layer is chemically etched to prevent direct contact between the two electrodes. To avoid short circuits, a compact thin film of TiO_2 is deposited on top of the conducting substrate to form a blocking layer between the hole-transport material and the fluorine-doped tin oxide. A mesoporous TiO_2 film composed of nanocrystalline particles (anatase) is layered on the blocking layer and sintered at a temperature of 450 °C for 30 min. Subsequently, the film is treated with a solution of $TiCl_4$ (20 mM in water) for 6 h and washed with distilled water. The film is then air-dried and sintered again at 450 °C for 45 min. The films are usually cooled from 450 °C to 80 °C and are then immersed into the dye solution for 10–12 h. The dye-stained films are rinsed with acetonitrile and dried in Ar flow.

A solution of spiro-OMeTAD (Figure 3) containing *tert*-butylpyridine and $Li(CF_3SO_2)_2N$ as additives is then applied on the porous film. After allowing the solution to permeate partially for 1 min, it is then spin-coated at 2000 rpm for 30 seconds to form the hybrid heterojunction. Back contact is applied by thermal evaporation of gold as the counter electrode. Details of the device fabrication can be found in references [40] and [41]. Upon light absorption, the sensitizer, which is anchored onto the mesostructured TiO_2 electrode, transfers electrons into the TiO_2. The sensitizer is in contact with the counter electrode through the organic hole-transport material spiro-OMeTAD, and the oxidized dye is regenerated by the holes in the hole-transport material.

3. Materials

3.1. Compact TiO_2

The role of the compact TiO_2 layer is to form a blocking interface between the fluorine-doped tin oxide and the hole-transport material. As these two materials form an ohmic contact,[42] it is crucial to have a compact layer that can impede the re-

combination of the electrons in the fluorine-doped tin oxide with the holes in the hole-transport material. This FTO/TiO_2/HTM junction requires a rectifying behavior to achieve a good performance of the device. A systematic study evaluating the merits of the blocking layer was published by Peng et al.[43] The compact TiO_2 layer is usually prepared by either sputtering,[43] chemical vapor deposition,[43,45] or sol-gel coating.[42] However, the blocking layers obtained by these processes are inferior to those obtained from spray pyrolysis.[47] Thelakkat et al. studied the effect of the thickness of the compact layer on the performance of solid-state DSSCs and concluded that a layer of 120–200 nm shows efficient rectifying behavior.[48] However, in our experience a better photovoltaic performance is obtained with a compact layer thickness of about 100 nm. Thicker films increase the series resistance which results in a lower fill factor. The current density is also lowered as a result of a thicker compact layer, as electron transport to the fluorine-doped tin oxide will be blocked. On the other hand, with thinner films there is an increased risk of direct contact between the fluorine-doped tin oxide and the hole-transport material owing to the unavoidable presence of pinholes. A Schottky barrier is also generated at the FTO/TiO_2 interface as a result of a high density of oxygen vacancies in the compact layer (a highly n-doped TiO_2) and obstructs the collection of electrons at the fluorine-doped tin oxide. This barrier reduces the performance of the solid-state DSSCs and demonstrates the importance of considering the interfacial property at the interface. It has been shown that the size of the Schottky barrier can be reduced by controlling the doping level during the deposition process, that is, by preventing the formation of a highly n-doped compact TiO_2 layer. The reduced barrier in turn improves the performance of the solid-state DSSC (e.g. from 2.1% to 3.7%[49,50]).

3.2. Mesoporous TiO_2

The high efficiency of DSSCs depends mainly on the nanocrystalline semiconductor film along with the dye spectral response.[51] The material of choice for the film is TiO_2 (anatase), although alternative wide-band-gap metal oxides such as ZnO[52,53] and SnO_2[54,55] have also been investigated. The high surface area of the mesoporous metal oxide film is critical for the efficient performance of the device as it allows strong absorption of the solar radiation by employing only a monolayer of adsorbed sensitizer. The use of a monolayer of dye prevents excited-state (or exciton) diffusion into the dye/metal oxide interface and also avoids the acceleration of non-radiative decay of the excited state to the ground state which is often associated with thicker dye films. The use of a mesoporous film results in a dramatic enhancement of the interfacial surface area (over 1000-fold for a 10-μm thick film) and leads to high absorbance of visible light from the monolayer of adsorbed dye (a dye monolayer adsorbed on a flat interface exhibits only negligible light absorption as the optical absorption cross-sectional areas for molecular dyes are typically two to three orders of magnitude smaller than their physical cross-section). The high surface area of such mesoporous films does, however, have a significant downside as it enhances the interfacial charge recombination at the TiO_2/sensitizer (or TiO_2/HTM) interfaces.

The mesoporous films used in solid-state DSSCs are composed of nanometer-size TiO_2 particles, which are prepared by hydrolysis of a metal–organic precursor (such as titanium isopropoxide), followed by peptization and hydrothermal treatment.[51] After dispersion of the colloidal particles in ethanol, terpineol and ethyl cellulose are added to the colloid and the mixture is then concentrated by a rotary evaporator to leave a paste for doctor-blading. Another facile route of making TiO_2 pastes from commercially available TiO_2 powder (P25, av. 30 nm, 80% anatase and 20% rutile; Degussa) which provides a suitable porous film for DSSCs was developed by our group.[56,57] An efficiency of 4% was observed for solid-state DSSCs fabricated using commercially available powders of TiO_2 with different particle sizes.[58]

3.3. Dyes and Other Light-Absorbing Materials

There are several basic requirements that guide the molecular engineering of an efficient sensitizer: 1) the excited-state redox potential should match the energy of the conduction-band edge of the semiconductor oxide; 2) light excitation should be associated with vectorial electron flow from the light-harvesting moiety of the dye towards the surface of the semiconductor surface to provide efficient electron transfer from the excited dye to the TiO_2 conduction band, strong conjugation across the electron donor and the anchoring groups of the sensitizer, and good electronic coupling between the lowest unoccupied molecular orbital (LUMO) of the sensitizer and the TiO_2 conduction band; 3) the highest occupied orbital (HOMO) of the sensitizer must be sufficiently low such that the oxidized dye is regenerated rapidly through electron donation from the electrolyte or a hole conductor; and 4) the sensitizer should be stable enough to sustain at least 10^8 redox turnovers under constant illumination, which corresponds to about 20 years of exposure to natural sunlight.[59]

In the early stages of development of solid-state DSSCs,[29,40,42] the red dyes N3 [*cis*-bis(isothiocyanato)-bis(2,2′-bipyridyl-4,4′-dicarboxylato)ruthenium(II)] and its partially deprotonated form N719 (Figure 2) were used as the light absorbers. By adding *tert*-butylpyridine and $Li(CF_3SO_2)_2N$ to the hole-transport material allowed the interfacial recombination processes to be controlled and an efficiency of 2.56% was achieved using an active cell area of 1.07 cm^2. This result was also confirmed at the National Renewable Energy Laboratories (Colorado, USA).[60] An improved efficiency was subsequently reached by using the silver complex of the sensitizer, which improved the open-circuit voltage (V_{oc}) and the dye uptake to give an efficiency of 3.2%.[61] The silver ion forms a complex with the sensitizer through the thiocyanate ligands, which results in a higher packing density of the sensitizer. The formation of the packed dye layer or the partial formation of a double dye layer thus leads to a better blocking of the dark current, and hence a higher open-circuit voltage.

Hydrophobic dyes were successfully applied to solid-state DSSCs leading to an overall efficiency of 4%.[37] In these cells, the hydrophobic alkyl chains improve the interfacial properties between the sensitizer and spiro-OMeTAD. The effects of these long chains and the kinetics of electron recombination on the device performance were studied.[62,63] It was inferred that certain lengths of alkyl chain retard the charge recombination at the interface by increasing the spatial separation between the TiO_2 and the hole-transport material.

Recently, another concept for the sensitizers was developed in our group: an ion-coordinating structure was introduced to the sensitizer (K51) to suppress charge recombination and improve the photovoltage of solid-state DSSCs.[64,65] The structure of K51 is similar to that of the well-known dye Z907 (Figure 4), except that the hydrophobic alkyl chains of Z907 are replaced by ion-coordinating triethylene oxide methyl ether groups, which suppress charge recombination. Solid-state DSSCs incorporated with K51 dye showed higher voltages than those containing the non-ion-coordinating analogue Z907.[64] K51 was further modified by adding heptyl groups to the ethylene oxide chains, which increased its hydrophobic properties while retaining its ion-coordinating properties (K68; Figure 4).[65] The function of Li^+ coordination at the back side of the sensitizer is to retard the recombination of electrons in TiO_2 and holes in the hole-transport material by a Coulombic screening effect at the TiO_2/dye/HTM interface.[38] Inclusion of the ion-coordinating sensitizer K68 in the solid-state device further slowed down the charge-recombination rate, resulting in significant improvements to the open-circuit voltage and the fill factor and an increase by approximately 20% in device efficiency relative to devices with Z907.[65] With the introduction of a strong reflector (Ag) as the counter electrode, solid-state DSSCs were obtained with efficiencies from 4.5% (illumination intensity 100 mW cm^{-2}) to 5.1% (illumination intensity 125 mW cm^{-2}).[66] Thus, molecular engineering of the sensitizers opens up a new horizon for organic–inorganic hybrid photovoltaic systems.

Another family of sensitizers that yields high efficiency is the donor-antenna series in which an electron-donor moiety such as triphenylamine or tetraphenylbenzidine is linked to the 2,2′-bipyridyl unit with π-extended conjugated bonding.[48,67,68] These functional structures utilize multiple-step charge-transfer cascades to impede the charge recombination. Moreover, the secondary triarylamine donor moiety, which displays a similar polarity to spiro-OMeTAD, is thought to improve the wetting behavior of the hole-transport material as it infiltrates into the porous TiO_2 film. Owing to the high molar extinction coefficients of the donor-antenna sensitizers, high current densities (9.6 mA cm^{-2}) at 77 mW cm^{-2} were obtained for the resulting solid-state DSSCs.

Organic dyes with high molar extinction coefficients are promising candidates for thin-film solid-state DSSCs. For example, an efficiency of 4.1% was obtained for a DSSC using an indoline dye, D102 (Figure 5).[69] Because of the strong molar extinction coefficient of this dye, a thin film of 1.6 μm was sufficient to achieve an efficiency of 4%. The high molar extinction coefficients of organic dyes make them ideal absorbers for solid-state DSSCs, although their photochemical stability requires further investigation. Another advantage of using organic dyes is the increased open-circuit voltages obtained relative to ruthenium complexes. The dye JK2 (Figure 5),[70] which was very successful in DSSCs containing liquid electrolytes, was used in a single-junction solid-state DSSC, which displayed an open-circuit voltage of over 1 V and a power conversion efficiency of over 3%.[71] This is the highest open-circuit voltage obtained to date for a solid-state DSSC device (its *I–V* characteristics are given in Figure 6 and Table 1). This high voltage may result from the dipole moment of these dyes. The influence of the dipole moment on the rectifying behavior was investigated by using various benzoic acids with different dipole moments,[72] and a model was proposed describing the effect of these dipole molecules on the work function of TiO_2 and on the energy levels across the TiO_2/dye/HTM interface. Experi-

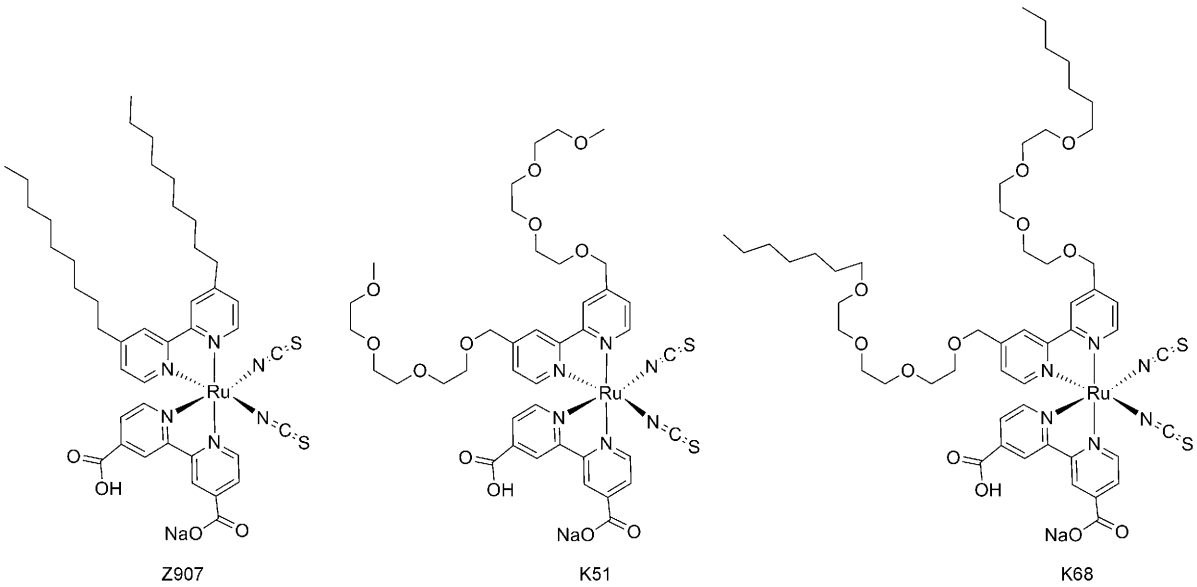

Figure 4. Structures of the dyes Z907, K51, and K68.

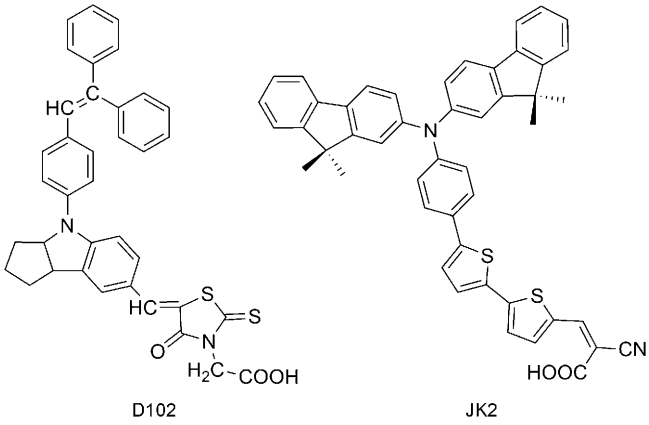

Figure 5. Structures of the organic dyes D102 and JK2 with high extinction coefficient.

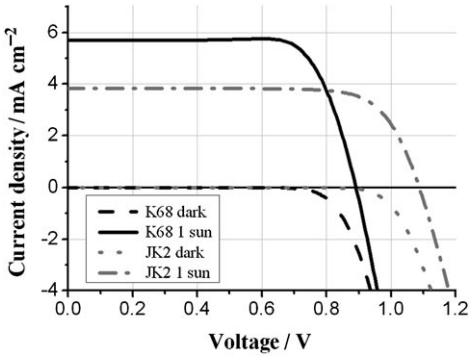

Figure 6. *I–V* characteristics of solid-state DSSCs with K68 or JK2 as dye and TiO_2 films containing 30-nm particles.

Table 1. Current–voltage parameters for the dyes shown in Figure 4.

Dye	V_{oc} [mV]	J_{sc} [mA cm^{-2}]	FF [%]	Efficiency [%]
JK2	1087.5	3.85	67.7	3.17
K68	896.7	5.7	76.1	3.88

mental results demonstrated that the dark current of a flat junction (TiO_2/dipole molecular/HTM) is suppressed as the dipoles point away from the TiO_2 surface. This dipole effect is likely to contribute to the high open-circuit voltages observed with organic dyes by offsetting the energy levels between the n-type TiO_2 and the p-type hole-transport materials.

Organic dyes that absorb in the red/near-IR range have also been successfully incorporated into solid-state DSSCs. In future these devices will contain different colored dyes and will therefore present a choice of colors for the photovoltaic modules. A solid-state DSSC based on green Zn-porphyrin dye (Figure 7) demonstrated an efficiency of 3%, a short-circuit current density of 5.9 mA cm^{-2}, and an open-circuit voltage of 790 mV.[73] A further shift of the absorption to longer wavelengths was achieved by using a blue squaraine dye, and the resulting solid-state DSSC displayed a short-circuit current density of 4.2 mA cm^{-2} and an overall efficiency of 1.5%.[74] The use of another blue dye, Zn-phthalocyanine PCH001 (Figure 7), resulted in a device efficiency of 0.87%, with a short-circuit current density of 2.1 mA cm^{-2}, an open-circuit voltage of 720 mV, and a fill factor of 0.52.[75] Although these dyes have narrow absorption bands, their high molar extinction coefficients facilitate the use of thin films without significant losses in light harvesting. The concept to extend light harvesting into the near-IR region is important with respect to complementary light absorption using dye cocktails (a combination of two dyes which complement each other in their spectral features) and tandem design.

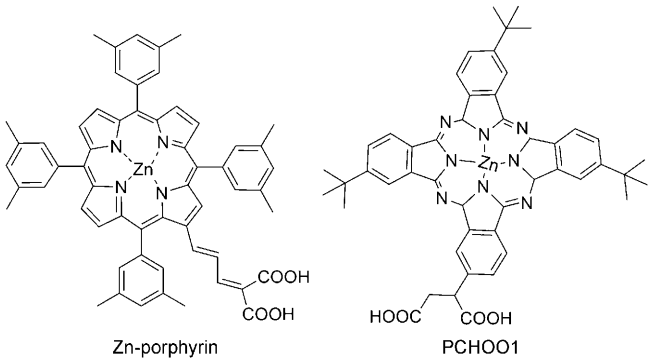

Figure 7. The red/near-IR-absorbing dyes Zn-porphyrin and Zn-phthalocyanine PCH001.

Quantum dots can also act as dye molecules to sensitize TiO_2, for example, PbS is an effective sensitizer for solid-state DSSCs.[76] Although the efficiency of devices that contain PbS is low (< 1%), it is encouraging that a semiconductor light absorber can operate well in an organic–inorganic heterojunction. Furthermore, there is evidence of multiple-exciton generation in quantum dots,[77] a concept which holds promise for the next generation of solar devices. However, a challenge remains concerning the fabrication of extra-thin absorber or quantum dot solar cells, that is, how to deposit uniformly the semiconductor light absorber onto the nanoporous matrix without losing its quantized features.

3.4. Hole-Transport Materials

The basic requirement for the hole-transport material is that its HOMO and LUMO levels are compatible with the HOMO level of the dye and the conduction band of TiO_2 to drive the charge-transfer process. In addition, the hole-transport material should be a transparent and amorphous thin film, as crystallization will prevent effective pore filling and thereby reduce its thermal and photochemical stability as well as carrier mobility. Inorganic p-type materials such as CuI[30,36] and CuSCN[33] are also possible candidates for hole-transport materials. Devices with these materials showed power conversion efficiencies of about 2%,[33,36] which was further improved to 3.8% by Meng et al. by using molten salt capped CuI.[78] The molten salt around the CuI not only controls the crystal size but also pro-

tects the CuI crystals from deterioration, thus improving the stability of the solid-state DSSC. Yanagida and co-workers introduced in situ photoelectrochemical polymerization of pyrrole[79] and 3,4-ethylenedioxythiophene[15] to obtain better pore filling.

Spiro-OMeTAD is by far the most successful p-type organic conductor (HTM). It displays a work function of about 4.9 eV and a hole mobility of $10^{-4}\,cm^2V^{-1}s^{-1}$.[80] The first reports on spiro-OMeTAD appeared in 1998, and the conversion yield of its devices has increased dramatically since then from less than 1% to over 5%.[37,66,68] The high efficiency stems from the inherent properties of spiro-OMeTAD, that is, its amorphous structure, good solubility, and small size. Spiro-OMeTAD is an organic non-crystalline molecule with a high glass-transition temperature, and its small size ensures solubility in organic solvents.

The presence of a lithium salt in spiro-OMeTAD influences the performance of the solid-state DSSCs; for example, doping with $Li(CF_3SO_2)_2N$ enhances the conductivity of spiro-OMeTAD and its hole mobility up to $1\times10^{-3}\,cm^2V^{-1}s^{-1}$.[50] Durrant and co-workers observed a 5–10-fold retardation of the interfacial recombination at HTM/TiO_2 upon addition of Li^+ salts,[81] whereas Thelakkat and co-workers reported an increase in the photocurrent and the photovoltage of the device.[48] Other triphenyldiamine hole-conductor derivatives with higher hole mobilities have been studied,[41] but none of them outperformed spiro-OMeTAD. Similar results were obtained with triarylamine hole-transport materials that do not contain a spiro linkage.[82,83] The presence of a spiro linkage improves the structural stability of the hole-transport material while maintaining its electronic properties. The perpendicular alignment of the two parts of the molecule presents a steric demand on their rigid structures, reducing the electronic interaction between the π systems and increasing the solubility of the spiro compound compared to their non-spiro-linked counterpart.[83] Although their electronic properties are better, non-spiro-linked hole-transport materials suffer from low pore filling.

It was reported recently that the intrinsic low hole mobility of spiro-OMeTAD does not limit the performance of solid-state DSSCs.[50,83] However, the charge recombination at the HTM/TiO_2 interface is usually much faster in solid-state DSSCs than in liquid electrolyte containing DSSCs.[85] Therefore, the recombination kinetics at the HTM/TiO_2 interface should be optimized as well as the pore filling of the hole-transport material in solid-state DSSCs. One way to overcome the difficulty of pore filling is to develop oxide films with regular mesoporous channels aligned perpendicular to the current collector. On the other hand, high open-circuit voltages (1 V) can be attained with these solid-state devices owing to a better match of the work function of the hole conductor (relative to that of electrolytes) with the redox potential of the sensitizer. Thus, the future of solid hole-conductor systems looks bright as long as the problems associated with charge recombination and pore filling of the hole-materials can be optimized.

4. Light Harvesting

Light harvesting is a key process for a good photovoltaic device. To enhance the scattering effect, bigger particles are introduced in the TiO_2 film to increase the optical path inside the porous matrix. A model was developed to analyze the optical process for the dye-absorbed TiO_2 films[86] and was applied to study the effect of light absorption with different particle sizes. It was found that larger particles with lower internal surface areas harvest more photons relative to smaller particles. The variation in absorbed flux $G(\lambda)$ as a function of wavelength is shown in Figure 8. The fluxes were calculated for a film

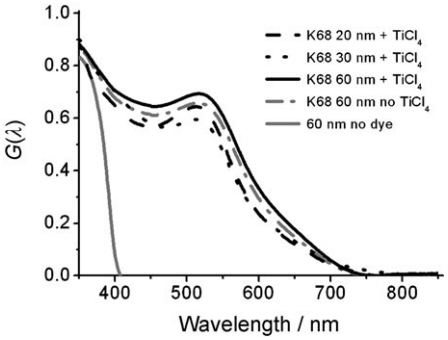

Figure 8. Variation of the absorbed flux (G) as a function of wavelength with 2.2-μm thick TiO_2 films containing differently sized TiO_2 particles (20–60 nm) and coated with K68 dye.

thickness of 2.2 μm, which is a typical value for solid-state DSSCs.[58] The observed absorption fluxes were higher for films composed of 60-nm particles compared to those composed of particles of 20 and 30 nm. A minor enhancement in the light absorption after $TiCl_4$ treatment is apparent. It is clear that the optical design of such thin films is far from optimum, as more than 30% of the light at the strong absorption region of the dye is usually lost. The light-harvesting efficiency in solid-state DSSCs is far from optimum in these 2-μm-thin films unless a very strongly light absorber is used. This non-optimum light-harvesting efficiency restricts the photocurrent output for the solid-state DSSCs to 8–10 $mA\,cm^{-2}$, which is almost 50% lower than those obtained from the most efficient DSSCs containing liquid electrolytes. One of the biggest challenges for solid-state DSSCs is to obtain good light harvesting although the thickness of the film (which is limited to the diffusion length of the charge) is shorter than the optical path length.

5. Interfacial and Electronic Properties

The heterojunction of solid-state DSSCs is a hybrid organic–inorganic interface. Several factors govern the performance of the device. The wetting of the hole-transport material on the dye-absorbed TiO_2 porous media is an important process to completely fill the tiny pores.[82] However, complete penetration of the hole-transport material into the pores is more critical than just wetting the surface of the nanoporous TiO_2, as a close contact between the dye and the hole-transport material

then facilitates the regeneration of excited dye molecules and enhances the active internal areas in such thin films. Long-term stability of the device may also be a concern if the pores are not completely filled.

Another important aspect concerning the modification of the interface is the co-adsorption of small molecules on TiO_2 to fill up the spaces between the dye molecules. This surface passivation prevents direct contact of the TiO_2 and the hole-transport material, where charge recombination happen easily. The effects of space filling, Coulombic screening, and dipole moment are all related to an improvement in the open-circuit voltage and electron lifetime in TiO_2. An enhancement in the open-circuit voltage has been observed with the co-adsorption of small molecules.[87–90] Improved open-circuit voltages as well as efficiencies were observed in solid-state DSSCs co-adsorbed dye and guanidinium-derived molecules.[41] As mentioned above, molecular engineering of the sensitizers is another example of interfacial modification. The ion-coordinating group in the sensitizer retards the recombination of the electrons in TiO_2 and the holes in the hole-transport material by a Coulombic screening effect at the TiO_2/dye/HTM interface and thus results in improved performances of solid-state DSSCs.[38]

The main drawback of solid-state DSSCs is the fast interfacial electron–hole recombination. The diffusion length of the conduction-band electrons is reduced to a few micrometers as compared to 20–100 μm for liquid electrolyte based DSSCs. The diffusion length (L_n), which is a key parameter for charge collection, is derived from $L_n = \sqrt{D_0 \tau_0}$, where D_0 and τ_0 represent the diffusion coefficient and lifetime of the electrons in the conduction band. The diffusion length thus calculated suggests that the thickness of the TiO_2 should be 2–3 μm. Recently, Peter et al. evaluated the diffusion length in solid-state DSSCs[91,92] by measuring the Fermi level with a third contact electrode on the TiO_2 film and calculated the diffusion length for solid-state DSSCs. Their results showed that the diffusion length is as high as 4.4 μm, significantly larger than the diffusion length determined previously.[85] This result implies that the thickness of the TiO_2 film is not a limiting factor for the efficiency of solid-state DSSCs. Also, this finding is encouraging because it suggests that if the pores of the TiO_2 matrix can be properly filled with the solid hole-transport material then a thicker film to increase light harvesting is achievable. The above results further indicate that interfacial engineering is a crucial factor for obtaining high-performance solid-state DSSCs in terms of charge recombination, physical separation of the charge-transport media, Coulombic screening, and offsetting the energy levels of the TiO_2 and the hole-transport material.

6. Summary and Outlook

Dye-sensitized mesoscopic injection solar cells have become a credible alternative to solid-state p–n junction devices. Such devices based on liquid electrolytes that contain the iodide/triiodide redox couple exhibit certified solar-to-electric power conversion efficiencies of 11%,[93] whereas solid-state DSSCs that incorporate solid-state hole-transport materials nowadays show power conversion efficiencies of around 5%. The improvements in the efficiency of solid-state DSSCs in recent years is attributed to 1) lower charge recombination at the FTO/TiO_2 interface by the introduction of a compact TiO_2 layer between the TiO_2 nanoparticles and the fluorine-doped tin oxide layer and 2) the enhanced hole mobility of the hole-transport material spiro-OMeTAD by doping with $Li(CF_3SO_2)_2N$. The hydrophobic alkyl chains in Ru-based sensitizers act as a blocking layer at the spiro-OMeTAD/TiO_2 interface, thereby reducing the back electron recombination. By incorporating ion-coordinating Ru-based sensitizers in solid-state devices, the performance of the devices can be improved by retarding the charge-recombination rate relative to devices using simple hydrophobic Ru-based sensitizers. The future of solid-state DSSCs thus looks bright, provided that the main drawbacks of pore filling and the fast recombination process at the interface can be addressed.

Presently, liquid electrolyte based DSSCs are at the point of commercialization (Figure 9). Their excellent performance in diffuse light gives them a competitive edge over silicon-based solar cells for stand-alone electronic equipments for both indoor and outdoor purposes. Thus, DSSCs offer many advantages over conventional solar cells, namely the low cost and low energy consumption of their production.

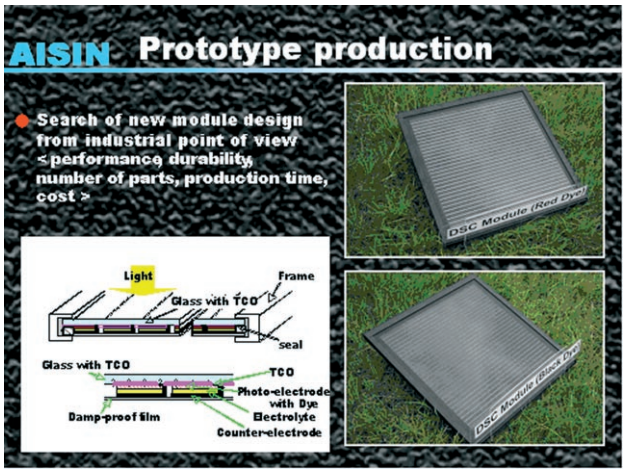

Figure 9. Production of DSSC prototypes by AISIN SEIKI (Japan). Note the monolithic design of the photovoltaic modules and the use of carbon as interconnecting and counter-electrode material. (Courtesy of AISIN SEIKI, Japan).

Acknowledgements

We thank CIME-EPFL for SEM measurements. P.C. acknowledges the Taiwan Merit Scholarship (TMS 094-2A-026) and J.-H.Y acknowledges Korea-Swiss GRL for financial support.

Keywords: energy conversion · materials science · sensitizers · solid-state dye-sensitized solar cells

[1] G. Yu, J. Gao, J. C. Hummelen, F. Wudl, A. J. Heeger, *Science* **1995**, *270*, 1789.
[2] J. J. M. Halls, C. A. Walsh, N. C. Greenham, E. A. Marseglia, R. H. Friend, S. C. Moratti, A. B. Holmes, *Nature* **1995**, *376*, 498.
[3] S. E. Shaheen, C. J. Brabec, N. S. Sariciftci, F. Padinger, T. Fromherz, J. C. Hummelen, *Appl. Phys. Lett.* **2001**, *78*, 841.
[4] W. U. Huynh, J. J. Dittmer, A. P. Alivisatos, *Science* **2002**, *295*, 2425.
[5] P. Peumans, S. Uchida, S. R. Forrest, *Nature* **2003**, *425*, 158.
[6] C. Lévi-Clément, R. Tena-Zaera, M. A. Ryan, A. Katty, G. Hodes, *Adv. Mater.* **2005**, *17*, 1512.
[7] F. Yang, K. Sun, S. R. Foresst, *Adv. Mater.* **2007**, *19*, 4166.
[8] B. O'Regan, M. Grätzel, *Nature* **1991**, *353*, 737.
[9] M. K. Nazeeruddin, S. M. Zakeeruddin, R. Humphry-Baker, M. Jirousek, P. Liska, N. Vlachopoulos, V. Shklover, C.-H. Fischer, M. Grätzel, *Inorg. Chem.* **1999**, *38*, 6298.
[10] J. B. Asbury, R. J. Ellingson, H. N. Gosh, S. Ferrere, A. J. Notzig, T. Lian, *J. Phys. Chem. B* **1999**, *103*, 3110.
[11] K. Hara, H. Sugihara, Y. Tachibana, A. Islam, M. Yanagida, K. Sayama, H. Arakawa, *Langmuir* **2001**, *17*, 5992.
[12] M. K. Nazeeruddin, P. Péchy, T. Renouard, S. M. Zakeeruddin, R. Humphry-Baker, P. Comte, P. Liska, C. Le, E. Costa, V. Shklover, L. Spiccia, G. B. Deacon, C. A. Bignozzi, M. Grätzel, *J. Am. Chem. Soc.* **2001**, *123*, 1613.
[13] F. L. Qiu, A. C. Fischer, A. B. Walker, L. M. Peter, *Electrochem. Commun.* **2003**, *5*, 711.
[14] M. K. Nazeeruddin, *Coord. Chem. Rev.* **2004**, *248*, 1161.
[15] Y. Saito, N. Fukuri, R. Senadeera, T. Kitamura, Y. Wada, S. Yanagida, *Electrochem. Commun.* **2004**, *6*, 71.
[16] N.-G. Park, M. G. Kang, K. M. Kim, K. S. Ryu, S. H. Chang, D.-K. Kim, J. Van de Lagemaat, K. D. Benkstein, A. J. Frank, *Langmuir* **2004**, *20*, 4246.
[17] R. Argazzi, G. Larramona, C. Contado, C. A. Bignozzi, *J. Photochem. Photobiol. A* **2004**, *164*, 15.
[18] J. Bisquert, D. Cahen, G. Hodes, S. Ruehle, A. Zaban, *J. Phys. Chem. B* **2004**, *108*, 8106.
[19] S. A. Haque, S. Handa, K. Peter, E. Palomares, M. Thelakkat, J. R. Durrant, *Angew. Chem.* **2005**, *117*, 5886; *Angew. Chem. Int. Ed.* **2005**, *44*, 5740.
[20] H. Lindstrom, A. Holmberg, E. Magnusson, S.-E. Lindquist, L. Malmqvist, A. Hagfeldt, *Nano Lett.* **2001**, *1*, 97.
[21] T. N. Murakami, Y. Kijitori, N. Kawashima, T. Miyasaka, *J. Photochem. Photobiol. A* **2004**, *164*, 187.
[22] J.-H. Yum, S.-S. Kim, D.-Y. Kim, Y.-E. Sung, *J. Photochem. Photobiol. A* **2005**, *173*, 1.
[23] S. A. Haque, E. Palomares, H. M. Upadhyaya, L. Otley, R. J. Potter, A. B. Holmesc, J. R. Durrant, *Chem. Commun.* **2003**, 3008.
[24] M. K. Nazeeruddin, F. De Angelis, S. Fantacci, A. Selloni, G. Viscardi, P. Liska, S. Ito, T. Bessho, M. Grätzel, *J. Am. Chem. Soc.* **2005**, *127*, 16835.
[25] M. Grätzel, *J. Photochem. Photobiol. A* **2004**, *164*, 3.
[26] Z.-S. Wang, T. Yamaguchi, H. Sugihara, H. Arakawa, *Langmuir* **2005**, *21*, 4272.
[27] Y. Chiba, A. Islam, R. Komiya, N. Koide, L. Han, *Appl. Phys. Lett.* **2006**, *88*, 223505.
[28] M. K. Nazeeruddin, T. Bessho, L. Cevey, S. Ito, C. Klein, F. De Angelis, S. Fantacci, P. Comte, P. Liska, H. Imai, M. Graetzel, *J. Photochem. Photobiol. A* **2007**, *185*, 331.
[29] U. Bach, D. Lupo, P. Comte, J. E. Moser, F. Welssörtel, J. Salbeck, H. Spreitzer, M. Grätzel, *Nature* **1998**, *395*, 583.
[30] K. Tennakone, G. R. R. A. Kumara, A. R. Kumarasinghe, K. G. U. Wijayantha, P. M. Sirimanne, *Semicond. Sci. Technol.* **1995**, *10*, 1689.
[31] B. O'Regan, D. Schwartz, *J. Appl. Phys.* **1996**, *80*, 4749.
[32] J. Hagen, W. Schaffrath, P. Otschik, R. Fing, A. Bacher, H. W. Schmidt, D. Haarer, *Synth. Met.* **1997**, *89*, 215.
[33] B. O'Regan, F. Lenzmann, R. Muis, J. Wienke, *Chem. Mater.* **2002**, *14*, 5023.
[34] R. Sanadeera, N. Fukuri, Y. Saito, T. Kitamura, Y. Wada, S. Yanagida, *Chem. Commun.* **2005**, 2259.
[35] J. Bandara, H. Weerasinghe, *Sol. Energy Mater. Sol. Cells* **2005**, *85*, 385.
[36] A. Konno, T. Kitagawa, H. Kida, G. R. A. Kumara, K. Tennakone, *Curr. Appl. Phys.* **2005**, *5*, 149.
[37] L. Schmidt-Mende, S. M. Zakeeruddin, M. Grätzel, *Appl. Phys. Lett.* **2005**, *86*, 013504.
[38] H. J. Snaith, S. M. Zakeeruddin, L. Schmidt-Mende, C. Klein, M. Grätzel, *Angew. Chem.* **2005**, *117*, 6571; *Angew. Chem. Int. Ed.* **2005**, *44*, 6413.
[39] B. Li, L. Wang, B. Kang, P. Wang, Z. Qiu, *Sol. Energy Mater. Sol. Cells* **2006**, *90*, 549.
[40] J. Krüger, PhD thesis, EPFL (Switzerland), **2003**.
[41] N. Rossier-Iten, PhD thesis, EPFL (Switzerland), **2006**.
[42] U. Bach, PhD thesis, EPFL (Switzerland), **2000**.
[43] B. Peng, G. Jungmann, C. Jager, D. Haarer, H. W. Schmidt, M. Thelakkat, *Coord. Chem. Rev.* **2004**, *248*, 1479.
[44] K. L. Hardee, A. J. Bard, *J. Electrochem. Soc.* **1977**, *124*, 215.
[45] M. Thelakkat, C. Shmitz, H.-W. Schmidt, *Adv. Mater.* **2002**, *14*, 577.
[46] C. D. Grant, A. M. Schwartzberg, G. P. Smestad, J. Kowalik, L. M. Tolbert, J. Z. Zhang, *Synth. Met.* **2003**, *132*, 197.
[47] L. Kavan, M. Grätzel, *Electrochim. Acta* **1995**, *40*, 643.
[48] C. S. Karthikezan, M. Thelakkat, *Inorg. Chim. Acta* **2008**, *361*, 635.
[49] H. J. Snaith, M. Grätzel, *Adv. Mater.* **2006**, *18*, 1910.
[50] H. J. Snaith, L. Schmidt-Mende, *Adv. Mater.* **2007**, *19*, 3187.
[51] C. J. Barbe, F. Arendse, P. Comte, M. Jirousek, F. Lenzmann, V. Shklover, M. Grätzel, *J. Am. Ceram. Soc.* **1997**, *80*, 3157.
[52] I. Bedja, P. V. Kamat, X. Hua, A. G. Lappin, S. Hotchandani, *Langmuir* **1997**, *13*, 2398.
[53] K. Keis, C. Bauer, G. Boschloo, A. Hagfeldt, K. Westermark, H. Rensmo, H. Siegbahn, *J. Photochem. Photobiol. A* **2002**, *148*, 57.
[54] Y. Tachibana, K. Hara, S. Takano, K. Sayama, H. Arakawa, *Chem. Phys. Lett.* **2002**, *364*, 297.
[55] A. N. M. Green, E. Palomares, S. A. Haque, J. M. Kroon, J. R. Durrant, *J. Phys. Chem. B* **2005**, *109*, 12525.
[56] S. Ito, P. Chen, P. Comte, Md. K. Nazeeruddin, P. Liska, P. Péchy, M. Grätzel, *Prog. Photovolt: Res. Appl.* **2007**, *15*, 603.
[57] Z. Zhang, P. Chen, T. N. Murakami, S. M. Zakeeruddin, M. Grätzel, *Adv. Func. Mater.* **2008**, *18*, 341.
[58] P. Chen, S. Ito, G. Rothenberger, M. Grätzel, unpublished results..
[59] *Future Generation Photovoltaic Technologies: Proceedings of the 1st NREL Conference* (March 22–26, 1997; Denver, Colorado), American Institute of Physics Conference Proceedings No. 404 (Ed.: R. D. McConnell), AIP, Woodbury, NY, **1997**.
[60] J. Krüger, R. Plass, L. Cevey, M. Piccirelli, M. Grätzel, U. Bach, *Appl. Phys. Lett.* **2001**, *79*, 2085.
[61] J. Krüger, R. Plass, M. Grätzel, *Appl. Phys. Lett.* **2002**, *81*, 367.
[62] L. Schmidt-Mende, J. E. Kroeze, J. R. Durrant, M. K. Nazeeruddin, M. Grätzel, *Nano Lett.* **2005**, *5*, 1315.
[63] J. E. Kroeze, N. Hirata, S. Koops, Md. K. Nazeeruddin, L. Schmidt-Mende, M. Grätzel, J. R. Durrant, *J. Am. Chem. Soc.* **2006**, *128*, 16376.
[64] D. Kuang, C. Klein, H. J. Snaith, J.-E. Moser, R. Humphry-Baker, P. Comte, S. M. Zakeeruddin, M. Grätzel, *Nano Lett.* **2006**, *6*, 769.
[65] D. Kuang, C. Klein, H. J. Snaith, R. Humphry-Baker, S. M. Zakeerudin, M. Grätzel, *Inorg. Chim. Acta* **2008**, *361*, 699.
[66] H. J. Snaith, A. J. Moule, C. Klein, K. Meerholz, R. H. Friend, M. Grätzel, *Nano Lett.* **2007**, *7*, 3372.
[67] C. S. Karthikeyan, H. Wietasch, M. Thelakkat, *Adv. Mater.* **2007**, *19*, 1091.
[68] C. S. Karthikeyan, K. Peter, H. Wietasch, M. Thelakkat, *Sol. Energy Mater. Sol. Cells* **2007**, *91*, 432.
[69] L. Schmidt-Mende, U. Bach, R. Humphry-Baker, T. Horiuchi, H. Miura, S. Ito, S. Uchida, M. Grätzel, *Adv. Mater.* **2005**, *17*, 813.
[70] S. Kim, J. K. Lee, S. O. Kang, J.-H. Yum, S. Fantacci, F. De Angelis, D. Di Censo, Md. K. Nazeeruddin, M. Grätzel, *J. Am. Chem. Soc.* **2006**, *128*, 16701.
[71] P. Chen, J. -H. Yum, S. J. Moon, M. K. Nazeeruddin, R. Humphrey-Baker, unpublished results.
[72] J. Krüger, U. Bach, M. Grätzel, *Adv. Mater.* **2000**, *12*, 447.
[73] L. Schmidt-Mende, W. M. Campbell, Q. Wang, K. W. Jolley, D. L. Officer. Md. K. Nazeeruddin, M. Grätzel, *ChemPhysChem* **2005**, *6*, 1253.
[74] A. Burke, L. Schmidt-Mende, S. Ito, M. Grätzel, *Chem. Commun.* **2007**, 234.
[75] Y. Reddy, L. Giribabu, C. Lyness, H. J. Snaith, C. Vijaykumar, M. Chandrasekharam, M. Lakshmikantam, J.-H. Yum, K. Kalyanasundaram, M. Grätzel, M. K. Nazeeruddin, *Angew. Chem.* **2007**, *119*, 377; *Angew. Chem. Int. Ed.* **2007**, *46*, 373.
[76] R. Plass, S. Pelet, J. Krueger, M. Grätzel, U. Bach, *J. Phys. Chem. B* **2002**, *106*. 7578.
[77] R. J. Ellingson, M. C. Beard, J. C. Johnson, P. Yu, O. I. Micic, A. J. Nozik, A. Shabaev, A. L. Efros, *Nano Lett.* **2005**, *5*, 865.

[78] Q.-B. Meng, K. Takahashi, X.-T. Zhang, I. Sutanto, T. N. Rao, O. Sato, A. Fujishima, *Langmuir* **2003**, *19*, 3572.
[79] K. Murakoshi, R. Kogure, Y. Wada, S. Yanagida, *Sol. Energy Mater. Sol. Cells* **1998**, *55*, 113.
[80] D. Poplavskyy, J. Nelson, *J. Appl. Phys.* **2003**, *93*, 341.
[81] T. Park, S. A. Haque, R. J. Potter, A. B. Holmes, J. R. Durrant, *Chem. Commun.* **2003**, 2878.
[82] L. Schmidt-Mende, M. Grätzel, *Thin Solid Films* **2006**, *500*, 296.
[83] J. E. Kroeze, N. Hirata, L. Schmidt-Mende, C. Orizu, S. D. Ogier, K. Carr, M. Grätzel, J. R. Durrant, *Adv. Func. Mater.* **2006**, *16*, 1832.
[84] T. P. I. Saragi, T. Spehr, A. Siebert, T. Fuhrmann-Lieker, J. Salbeck, *Chem. Rev.* **2007**, *107*, 1011.
[85] J. Krüger, R. Plass, M. Grätzel, *J. Phys. Chem. B* **2003**, *107*, 7536.
[86] G. Rothenberger, P. Comte, M. Grätzel, *Sol. Energy Mater. Sol. Cells* **1999**, *58*, 321.
[87] P. Wang, S. M. Zakeeruddin, R. Humphry-Baker, J. E. Moser, M. Grätzel, *Adv. Mater.* **2003**, *15*, 2101.
[88] P. Wang, S. M. Zakeeruddin, P. Comte, R. Charvet, R. Humphry-Baker, M. Grätzel, *J. Phys. Chem. B* **2003**, *107*, 14336.
[89] Z. Zhang, S. M. Zakeeruddin, B. C. O'Regan, R. Humphry-Baker M. Grätzel, *J. Phys. Chem. B* **2005**, *109*, 21818.
[90] J.-H. Yum, S.-R. Jang, R. Humphry-Baker, M. Grätzel, J.-J. Cid, T. Torres, M. K. Nazeeruddin, *Langmuir* **2008**, *24*, 5636.
[91] J. R. Jennings, L. M. Peter, *J. Phys. Chem. C* **2007**, *111*, 16100.
[92] L. M. Peter, *J. Phys. Chem. C* **2007**, *111*, 6601.
[93] M. A. Green, K. Emery, Y. Hisikawa, W. Warta, *Prog. Photovolt: Res. Appl.* **2007**, *15*, 425.

Received: April 18, 2008
Published online on July 10, 2008

